# IAEA CRP on HTGR Uncertainties: Sensitivity Study of PHISICS/RELAP5-3D MHTGR-350 Core Calculations using Various SCALE/NEWT Cross-Section Sets for Ex. II-1a

Pascal Rouxelin[1]*, Gerhard Strydom[2], Andrea Alfonsi[2], Kostadin Ivanov[1]

[1]*North Carolina State University, 2500 Stinson Drive, Raleigh, NC, 27606, pnrouxel@ncsu.edu*
[2]*Idaho National Laboratory, 2525 Fremont Avenue, Idaho Falls, ID, 83415.*
** Corresponding Author*

*Uncertainty and sensitivity analysis is an indispensable element of any substantial attempt in data validation. The quantification of uncertainties in nuclear engineering has grown more important and the IAEA Coordinated Research Program (CRP) on High-Temperature Gas Cooled Reactor (HTGR) initiated in 2012 aims to investigate the various uncertainty quantification methodologies for this type of reactors. The first phase of the CRP is dedicated to the estimation of uncertainties due to the neutron cross sections. Phase II is oriented towards the propagated uncertainties from the lattice to the coupled neutronics/thermal hydraulics core calculations. Nominal results for the prismatic single block (Ex.I-2a) and super cell models (Ex.I-2c) have been obtained using the SCALE 6.1.3 two-dimensional lattice code NEWT coupled to the TRITON sequence for cross section generation. It is proposed to utilize the TRITON/NEWT-generated, flux-weighted cross sections obtained through Ex.I-2a, and various models of Ex.I-2c, to perform a sensitivity analysis on the MHTGR-350 core modeled with the INL coupled code PHISICS/RELAP5-3D, utilizing a fixed temperature feedback for Ex. II-1a. The power density distribution is evaluated at different radial and axial locations and compared between the different core models. It is observed that the core power density does not vary significantly in shape, but the magnitude of the variations increases as the moderator-to-fuel ratio in the super cell generated with TRITON/NEWT increases.*

## I. Introduction

The continued development of High-Temperature Gas-Cooled Reactors (HTGRs) requires verification of HTGR design and safety features with reliable high-fidelity physics models as well as robust, efficient, and accurate codes. HTGRs take the form of two operational fuel types: the pebble bed and the cylindrical compact (or rod) embedded in a hexagonal fuel block, as for example used in the Modular High Temperature Gas-cooled Reactor (MHTGR). Both fuel types are characterized by several peculiarities in contrast to LWRs. The main difference remains the double heterogeneity of the fuel elements. In both configurations, the heavy metal kernel (usually $UO_2$, but also UCO or UCN) is located in the inner part of Tri-structural (TRISO) coated particles. These particles are scattered in a graphite matrix to constitute either the pebbles surrounded with pure graphite, or the cylindrical compacts. Therefore, the resulting models are in a double heterogeneous state, the first heterogeneity being the kernel in the TRISO particle while the second one is the TRISO particles in the graphite matrix.

The IAEA launched a Coordinated Research Program (CRP) on HTGR Uncertainty Analysis Modeling (UAM) [1] to investigate uncertainty propagation and ensure the continuation of methods and simulation development of HTGRs. In a separate effort, the OECD/NEA MHTGR-350 MW benchmark [2] was launched at Idaho National Laboratory (INL) in 2012 to provide a best-estimate code-to-code verification data set for the development of HTGR tools. The general approach of both benchmarks is to define various phases and exercises, corresponding to the typical cell, lattice and core simulation requirements, and using common data sets. The CRP on HTGR utilizes the same MHTGR-350 design information specified in the OECD/NEA MHTGR-350 benchmark for the cell and lattice phases, and the core models developed for the latter benchmark can therefore also be applied to the CRP Phase II and III problems.

The first Phase of the HTGR UAM is dedicated to neutronics calculations, ranging from lattice cells (Exercise (Ex.) I-1a/b) to single block (Ex. I-2a/b) and supercell (Ex.I-2c) calculations. It is aimed in a first place to evaluate cross-section and material input uncertainties, but later on also comparing the cross section libraries generated in Phase I for use in the Phase II core models. The 2-D deterministic code NEWT, included in SCALE 6.1.3 was used for the cross section generation into AMPX-formatted nuclear data libraries. It is proposed in this project to evaluate the effects of using single block and supercell lattice models for the generation of few-

group core cross sections. The neutronics core solutions for steady state are obtained using the 238-group NEWT cross section libraries collapsed to a 26-group format. The 26-group core solutions are calculated with the INL code suite PHISICS (Parallel and Highly Innovative Simulation for INL Code System) coupled to the INL system thermal hydraulics code RELAP5-3D (section II.B). In this study, the PHISICS/RELAP5-3D axial and radial power profiles are evaluated to measure the effect of the various flux-weighted neutron cross section sets on the core solutions.

## II. Description of the codes

This section provides an overview of the deterministic lattice code SCALE/NEWT. The coupled PHISICS/RELAP5-3D code utilized for the Phase II calculations is also described.

### II.A. Cross section generation: NEWT/TRITON (SCALE6.1) lattice calculations

The NEWT transport solver of the SCALE 6.1 package, developed at the Oak Ridge National Laboratory (ORNL), is a multi-group discrete-ordinates transport computer code characterized by flexible meshing features that allow complex geometric models. The NEWT computational approach is based on refined approximation of curves and irregular surfaces and therefore can represent models that would normally be highly impractical to design with $S_n$ ordinate methods. NEWT is used to determine the nominal (i.e. best-estimate) eigenvalues for Exercises I-2(a, b and c), and to generate the collapsed multi-group, flux-weighted microscopic AMPX cross-section libraries for use in the PHISICS/RELAP5-3D solution of Exercise II-1a.

Although NEWT can be used as a stand-alone neutron transport solver, SCALE 6.1.3 provides the ability to include NEWT in a SCALE/TRITON (Transport Rigor Implemented with Time-dependent Operation for Neutronics depletion) sequence to prepare the homogenized, flux-weighted nuclear data. In the 6.1 version of SCALE, the double heterogeneous configuration of prismatic lattices is still a limitation to the TRITON capabilities, especially in terms of SA and UA.

### II.B. Core steady-state calculations PHISICS/ RELAP5-3D

The transport solver PHISICS has been coupled to the INL system thermal-hydraulics code RELAP5-3D. PHISICS is a neutronics code system [3] in development at INL since 2011, and recent updates provided a very capable and flexible platform to cope with the challenges of coupled-neutronics/thermal-hydraulic MHTGR core simulations. The different modules for PHISICS are a nodal and semi-structured spherical-harmonics-based transport core solver (INSTANT) for steady-state and time-dependent problems, a depletion module (MRTAU), and a cross-section mixer-interpolator (MIXER) module.

The RELAP5-3D code has been developed for best estimate transient simulation of light water reactor coolant systems during postulated accidents, but the generic modeling approach allows HTGR simulations as well. The code integrates the coupled behavior of the reactor coolant system and the core for loss-of-coolant accidents. Anticipated transient without scram can be modeled, for instance loss of offsite power, or loss of flow accidents. In this study, the PHISICS/RELAP5-3D "ring" model of the MHTGR-350 design [4] was used to provide a constant isothermal temperature of 1200 K to the neutronics module for the steady-state solution, as prescribed in the draft specification for Phase II-1a.

## III. Description of the neutronics model

A representation of a two-dimensional TRISO particle cut at the center is shown in Fig. 1. The TRISO particles are scattered randomly over fuel compacts embedded in prismatic blocks.

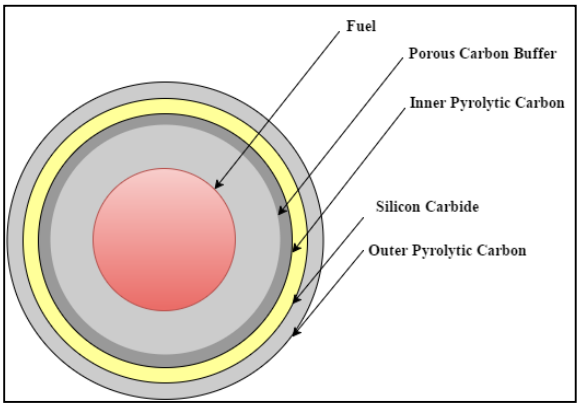


Fig. 1. TRISO particle representation in a centered two-dimensional cut

Coolant channels are alternatively dispatched over the prismatic configuration to remove the heat out of the fuel. Six burnable poison (BP) rods are located at the corners fresh fuel block. Fuel coolant and burnable poison channels are surrounded by graphite moderator. A picture of a fresh MHTGR-350 fuel block prismatic block is showed in Fig. 2. The two-dimensional feature of NEWT does not provide capabilities to model explicitly the burnable poison coated particles.

It has been chosen to smear out the particles containing the burnable absorbers for the generation of the cross section data with NEWT/TRITON.

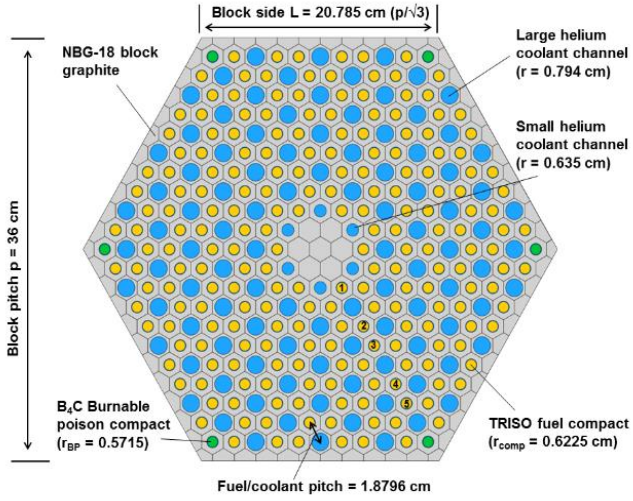


Fig. 2. Radial representation of a fresh prismatic block

The burned MHTGR-350 fuel block is identical to the fresh block, but without any of the burnable poisons compacts remaining. A second model has been developed in the form of a seven-block "super cell" to capture the neutron flux spectral effects more accurately over the blocks. It consists in a heterogeneous block as described in Fig. 2 surrounded above and below by two homogeneous regions representative of the core pattern [5]. A typical super cell is represented in Fig. 3. The purpose of this model is, as mentioned earlier, to generate cross section data based on the different neutron spectrum observed locally in the MHTGR-350 core (see Fig. 4).

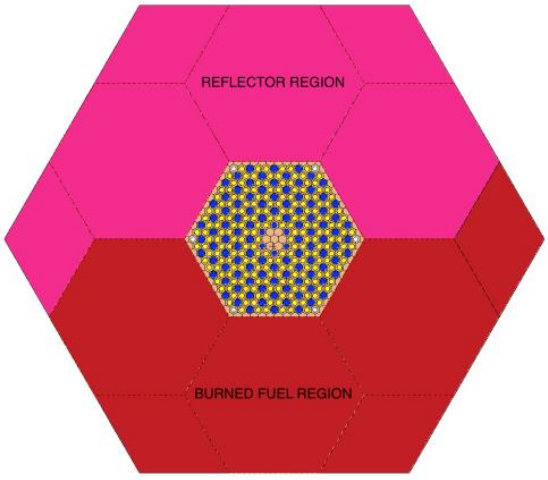


Fig. 3. Design of a super cell (Ex. I-2c)

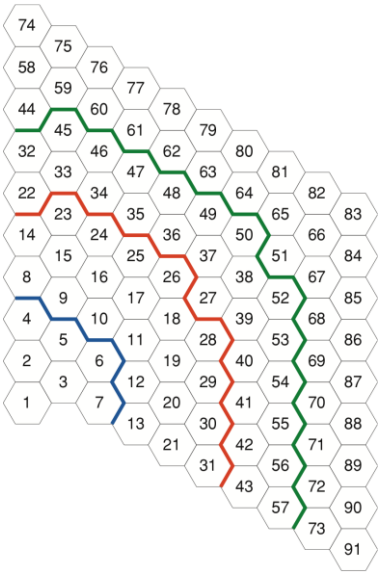

Fig. 4. MHTGR-350 third core representation. Blocks 1 through 7, 22, 27 and 32 to 91 are reflector blocks. Blocks 8 through 21, 23 through 26 and 28 through 31 are fuel blocks

It is intended for example to investigate the neutron flux effects at the periphery of the fuel ring (i.e. blocks 8 through 13, blocks 23 through 26 and block 28 through 31) versus the neutron flux in the central fuel belt in the core (blocks 14 through 21). Note that only the central block's cross section data are collected from the super cell, and not the cross sections characterizing the entire super cell.

Overall, in a case of a mixed core made of burned and fresh blocks, a set of about fifteen super cells can be constructed [6]. Due to space limitations, only the results obtained for the fresh-fuel super cells are presented. An additional super cell is defined to generate cross section data for the reflector to represent the inner region, outer region and replaceable graphite moderator around the fuel blocks.

Two lattice representations are used to generate the nuclear cross sections for later use in the PHISICS-RELAP5-3D core calculation. The first one (referred as to exercise I-2a in the benchmark specifications) is a single fuel block surrounded by reflective boundary conditions, as depicted in Fig. 2. Exercise I-2a is used as reference to compare with the super cell models, since this is the most basic (and for most historical applications the default) lattice representation. The second system is a set of four super cells having a fresh fuel block at the center (see Fig. 5). In the figure, the plain pink blocks are homogenized fresh fuel (labelled "A") and the striped pink blocks heterogeneous fresh fuel, and the black blocks represent reflector graphite (labelled "R").

The four super cells are referred to as super cell *k* (three graphite blocks), super cell *l* (two graphite blocks), super cell *m* (one graphite block) and super cell *i* (no graphite block). In these cells, the $^{10}B$ and $^{11}B$ in the BPs have been removed from the fuel homogenized regions to prevent an artificial self-shielding effect during the homogenization of the blocks.

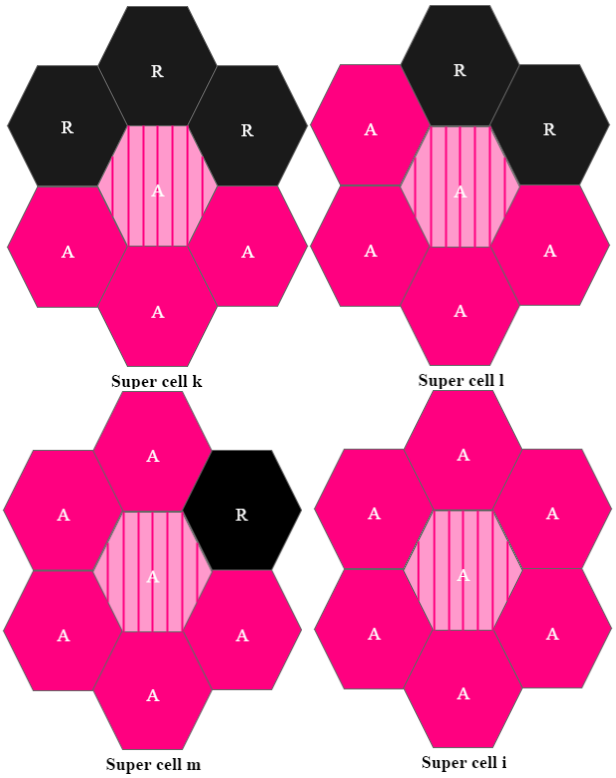


Fig. 5. Representations of the Ex. I-2c super cells k, l, m and i.

## IV. Neutron flux across the central block in the super cells

The normalized neutron flux per unit lethargy across the central block of the super cells *i*; *m*; *l*; *k* is given in Fig. 6. The neutron flux is given in a 26-group structure [7]. The super cell *k* contains the local region that has highest moderation achievable in the core design, thus providing the softest (most thermal) flux. The single block (Ex. I-2a) does not have additional reflector blocks surrounding it and thus represents the lowest moderator-to-fuel ratio. The super cells differ from each other by the isotopic composition of the two homogenized regions located around the heterogeneous central region.

The neutron spectrum at the center of the super cell becomes more thermal as the amount of graphite increases. It has been shown that the topology of the homogenized regions around the heterogeneous central block does not influence the neutron flux spectrum at the center of the super cell greatly [6].

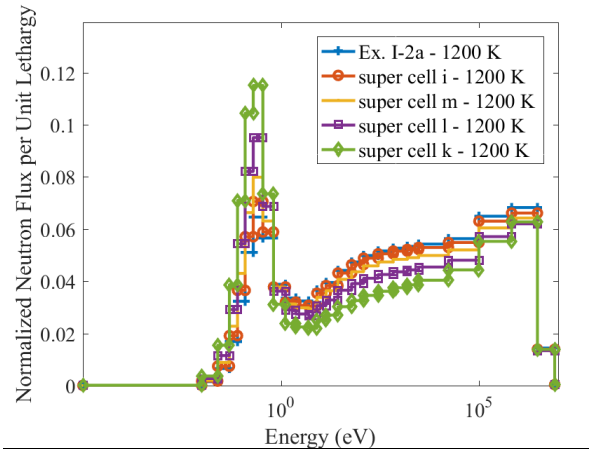


Fig. 6. Normalized neutron flux per unit lethargy in 26-group structures for Ex. I-2a and Ex. I-2c super cells i, m, l and k.

A neutron flux map is provided for each model to illustrate the differences between the super cells in Fig. 7 for group 3 (the fast group with the highest chi). It should be noted that the color code is relative to each model, i.e. it should not be cross-compared between the various cells. The neutron flux appears to be especially homogeneous and hard in the heterogeneous portion of super cell k, since there are very few neutrons in group 3 crossing the north region in this cell's graphite region, which implies that group 3 is well represented throughout the central block as compared to the north region. The super cells *i* and the single block 2a have the same isotopic composition, accounting for the fact that the boundaries are reflective.

It can be observed from Fig. 6 and Fig. 7 that Ex. I-2a and the heterogeneous block in super cell *i* have similar neutron fluxes. Super cell *l* illustrates the spatial spectrum effect induced by the super cell: the spectrum in the northern section of the heterogeneous block is harder than in the southern section. This suggests that the fission rate is greater at the top than the bottom part of the super cell due to the locally better moderation. The flux differences induced by the super cell configuration modify the flux weighting of the nuclear cross sections.

The product of the normalized neutron flux per unit lethargy and the homogenized microscopic cross section (i.e. reaction rate) originating from the central block in super cells *i* and *k* are compared with the single block reaction rate in Fig. 8. It is confirmed in Fig. 8 that the reaction rates originating from thermal regions (at the periphery of the core) are significantly different to the reaction rates at the center of the core where the neutron flux is harder.

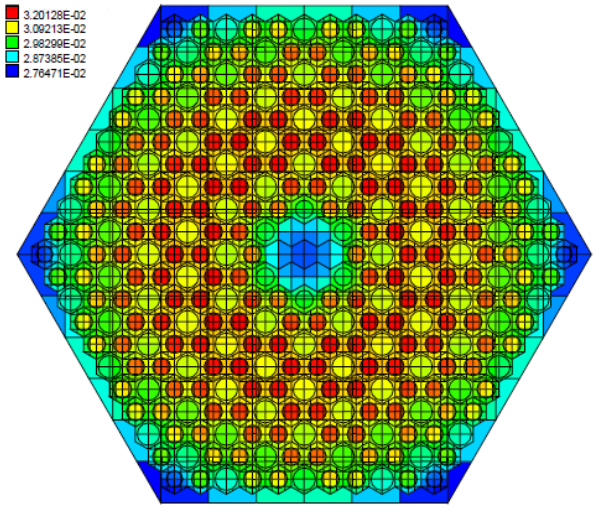


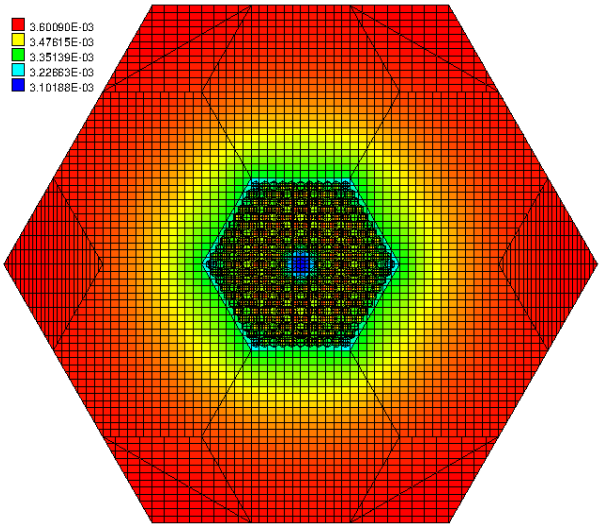


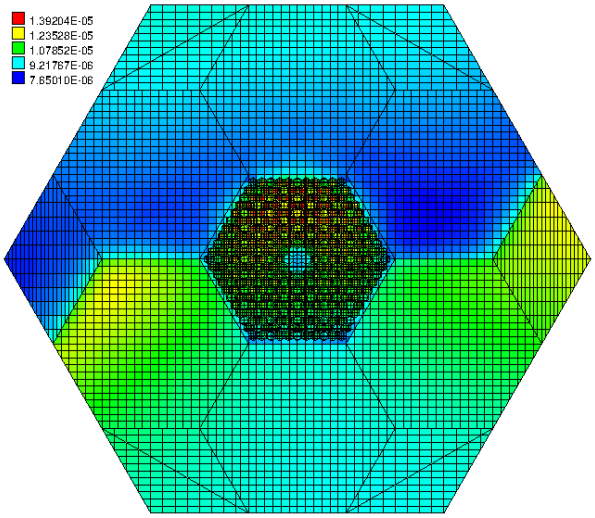


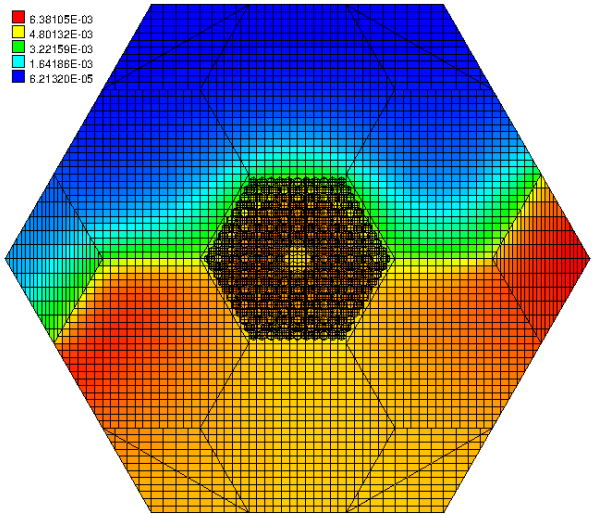


Fig. 7. Neutron flux maps in group 3 for Ex. I-2a and Ex. I-2c super cells *i*,*l* and *k* respectively.

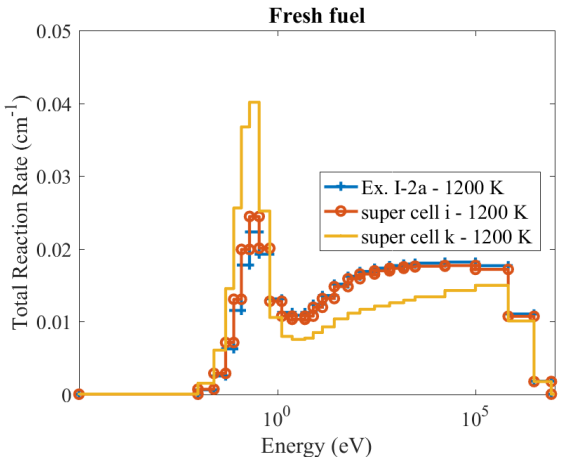


Fig. 8. "Normalized" total reaction rates for Ex. I-2a and Ex. I-2c super cells i and k.

## V. PHISICS/RELAP5-3D core calculations

In this section, the influence of the various flux-weighted cross sections originating from the super cells is evaluated when these 26-group data sets are implemented in the PHISICS/RELAP5-3D core calculations.

### V.A. Description of the model

The flux weighted AMPX-formatted 26-group cross sections are used as input to the homogenized one-third core model on a block-by-block basis. The PHISICS/RELAP5-3D core model constructed with the cross sections generated from Exercise I-2a is depicted in Fig. 9 (hereafter referred to as "core 2a"). Core *2a* is used as a reference case for comparison with more complex core configurations.

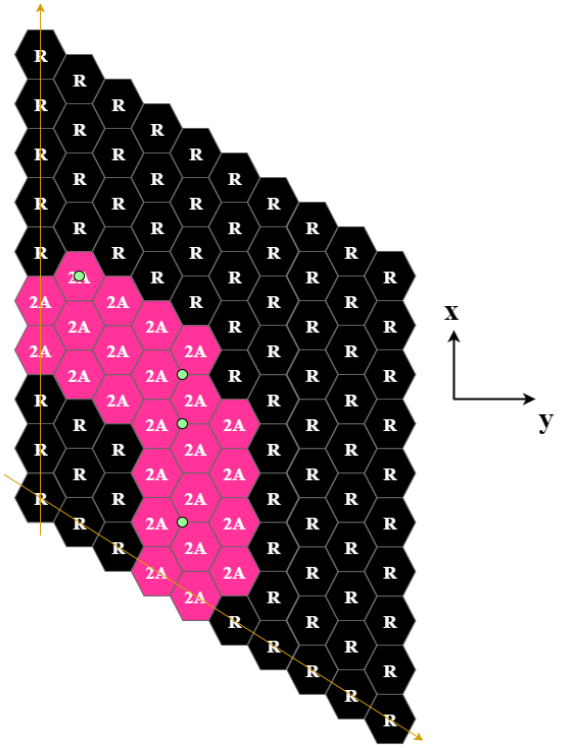


Fig. 9. PHISICS/RELAP5-3D third core packed with Ex. I-2a cross sections

This core represents the simplest link between the lattice and core simulation phases, as it only utilizes cross sections generated by a single infinitely-reflected fuel block. It is intended to evaluate the effects induced by the implementation of the cross sections that were generated previously (Section IV) according to their local spectral environment. The super cell *k*'s cross sections are utilized for instance at the periphery of the core as shown in Fig. 10 in core *i; k; l; m*. The reflector blocks utilize the same cross section set throughout the core.

The results obtained for four PHISICS/RELAP5-3D cores are reported in this study (in order of complexity): the reference core *2a*; a core loaded with the cross sections *i*, a core using the cross section sections flux-weighted with the most thermal neutron flux (core *k*), and the most refined core using the cross section originating from super cells *i*, *k*, *l*, *m*. The 26-group NEWT microscopic cross sections are collapsed from the 238-group structure and stored in the AMPX format. The PHISICS input utilizes the homogenized isotopic inventory to perform the flux and criticality calculations.

The effective multiplication factor computed by PHISICS for each cores is summarized in Table I. The multiplication factor increases as the neutron flux softens in the NEWT/TRITON models. The k-effective differences between the four super cell models are relatively small (less than 200 pcm between the "softest" and "hardest" set). A detailed investigation of reaction rates and flux distributions would be required to fully assess the effects of these different cross section sets; in this paper, the integral effects on the power density profiles are compared in Section V.B.

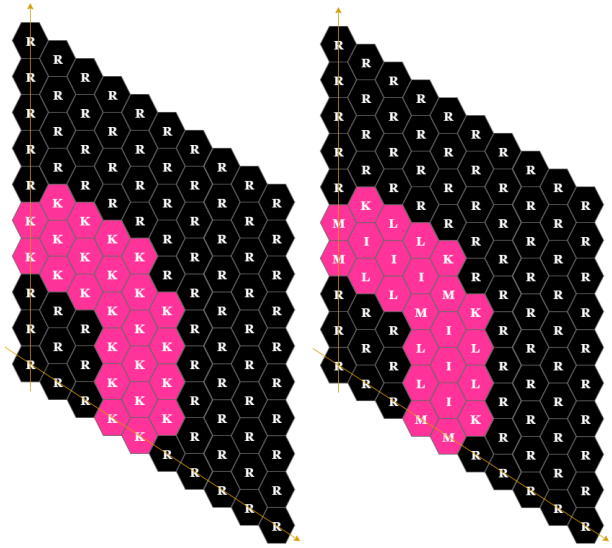

Fig. 10. PHISICS/RELAP5-3D one-third core models constructed with Ex. I-2a and Ex. I-2c super cell *k* (left) and cells *k*, *l*, *m*, and *i* (right) cross sections

TABLE I. Effective multiplication factor obtained in PHISICS with the NEWT AMPX-formatted microscopic cross sections

| Core loadings | k-effective | Absolute Difference (pcm) |
|---|---|---|
| 2a | 1.39849 | (reference) |
| i | 1.39753 | -96 |
| i-k-l-m | 1.39902 | 53 |
| k | 1.39955 | 106 |

### V.B. Axial power density profiles

The axial power density profile is evaluated at four different radial locations indicated by the green dots in Fig. 9, as indicated in Table II.

TABLE II. Radial coordinates of the points selected for the axial power density profile comparison

| Point number | x-coordinates (cm) | y-coordinates (cm) |
|---|---|---|
| 1 | 54.0 | 93.53 |
| 2 | 126.0 | 31.17 |
| 3 | 90.0 | 93.53 |
| 4 | -18.0 | 93.53 |

The power density profiles are presented for core *2a* in Fig. 11. It can be observed that the highest power densities are located in the inner parts of the fuel ring. The points 2 (yellow line with dotted markers) and 3 (purple

line with circled markers) presented in Table II are overlapping in the axial power profile figure. The power is zero at the top and the bottom graphite reflector region. It can also be observed that there is a slight peak at the axial fuel-moderator boundary. This peak is due to the local higher moderator-to-fuel ratio, and is more pronounced at points 2 and 3, where the fuel blocks are located next to the graphite blocks radially.

A comparison of the axial power density profiles for the four core models at the periphery of the core (x=126.0 cm; y=31.1 cm, north-most green dot in Fig. 9) is shown in Fig. 12.

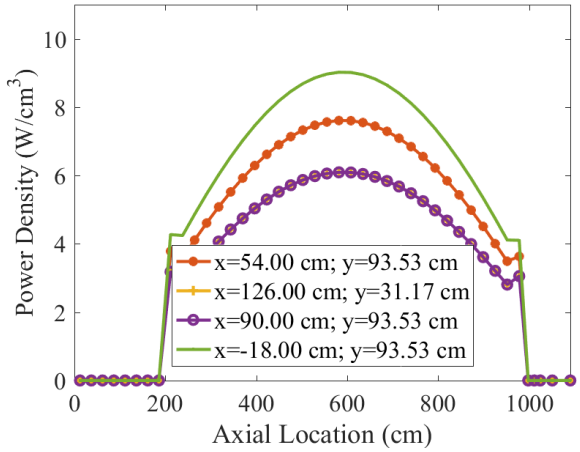


Fig. 11. Axial power density profile for Core *2a*

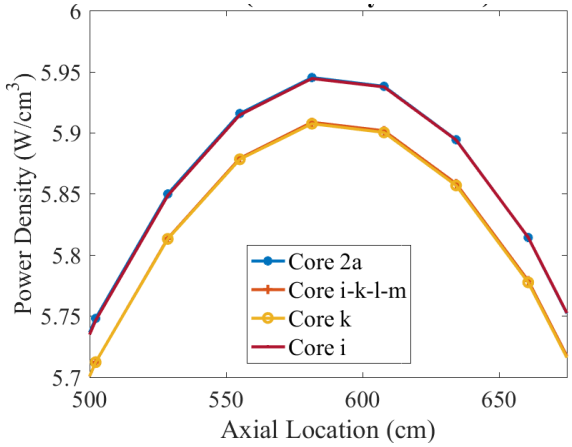


Fig. 12. Comparison of the axial power density profiles between core *2a*; *i-k-l-m*; *k* and *i* at the radial coordinates x=126 cm; y=31.7 cm

No differences are observed between cores *2a* and *i*. Likewise, no significant differences exist at periphery of the fuel ring between the core *k* and the most refined core *i-k-l-m*, since the central block evaluated is filled with the same cross section (super cell *k*) in both core *k* and core *i-k-l-m*. Note that the number densities are identical for the cores of interest. Therefore, the slight difference between core *2a* and *k* (or *i-k-l-m*) is induced by the cross sections that are flux-weighted during the NEWT/TRITON sequence.

### V.C. Power density distribution

In this section, the radial power densities of the super cell cores are compared to the reference core *2a* at the axial location z=607.9 cm, corresponding to the peak power density. The comparison of core *2a* with core *i* (Fig. 13) shows no significant impact of these flux-weighted cross sections on the power density distribution.

The power density map of the differences between core *i-k-l-m* and core *2a* (Fig. 14), as well as between core *k* and core *2a* (Fig. 15) show that the implementation of the various cross section sets pushes the power density towards the edges of the cores. This effect is compensated at the center of the fuel region by a decrease in the power density. The relative power density differences are similar in cores *i-k-l-m* and *k*. The largest differences are observed in the center region.

It is important to notice that the use of the libraries *i* in the core *i-k-l-m* still results in a -0.8% difference, although these cross sections do not change the power distribution in the core *i*. This implies that the use of cross sections flux weighted with a soft spectrum (super cell k or l) leads to a flux redistribution, and the heat increase on the periphery of the core is balanced with a reduction in the center region. The overall trend is identical for the *i-k-l-m* and *k* cores, although slightly more pronounced in the case of core *k*. This suggests that the more complex set of cross sections *i-k-l-m* only lead to a slight modification of the power density distribution.

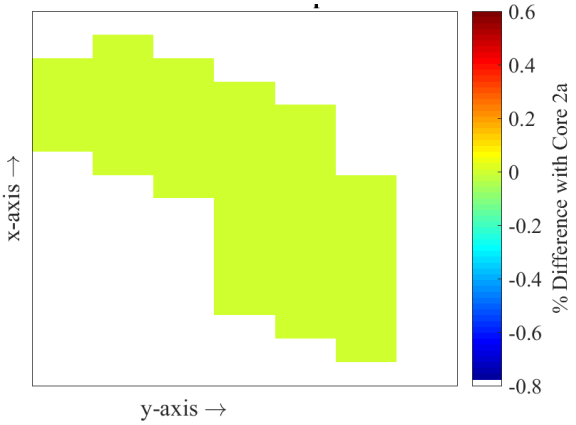


Fig. 13. Power production relative difference (%) between the core *i* and core *2a* (reference)

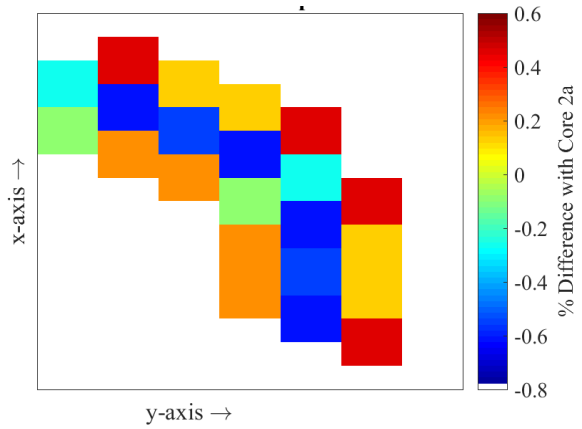


Fig. 14. Power production relative difference (%) between the core *i-k-l-m* and core *2a* (reference)

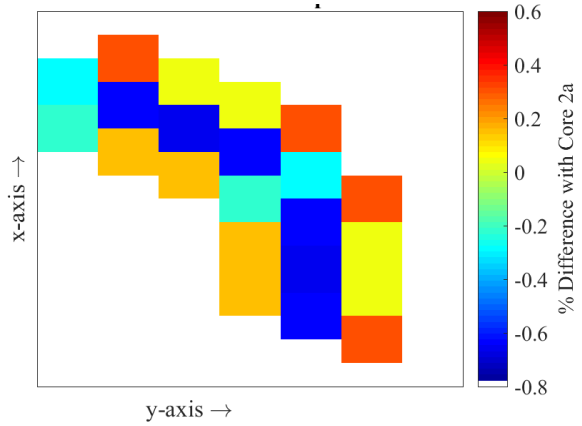


Fig. 15. Power production relative difference (%) between the core *k* and core *2a* (reference)

## VI. CONCLUSIONS

The neutron flux spectra in super cells are strongly influenced by the amount of graphite in the system. This in turn induces significant variations in the flux-weighted nuclear cross sections. It has been shown in this study that the subsequent use of these super cell lattice cross sections in 26 group MHTGR-350 PHISICS/RELAP5-3D core calculations has a minor impact on the full core steady state multiplication factor (less than 200 pcm) and the radial and axial power density profiles. At the center of the core, the power density changes are limited to 0.8% (in absolute value) compared to a reference core loaded with the cross sections originating from an infinitely-reflected single fuel block (Ex I-2a).

The evaluation of differences obtained with two super cell lattice models applied to cores *i-k-l-m* and core *k* suggest that the use of a softer spectrum super cell leads to a minor redistribution of the power profiles. The use of super cell *i-k-l-m* cross sections does not change the results significantly, which implies that the generation of cross sections using more complex super cells is probably not required for these core calculations. The use of soft super cell libraries is sufficient to induce the observed power redistribution. It must however be kept in mind that these conclusions are based on the current 26-group PHISICS structure, and that a lower number of groups (e.g. less than 8) could lead to more significant spectral differences between these models.

## AKNOWLEDGMENTS

This work was prepared for the U.S. Department of Energy Office of Nuclear Energy under DOE Idaho Operations Office Contract DE-AC07-05ID14517.

## REFERENCES

1. F. REITSMA, G STRYDOM, F. BOSTELMANN, K IVANOV, "*The IAEA Coordinated Research Program on HTGR Uncertainty Analysis: Phase I Status and Initial Results*", Proc. of HTR2014, Kyoto, Japan, American Nuclear Society (2014).
2. J. ORTENSI, et al., "Prismatic Coupled Neutronics/Thermal Fluids Transient Benchmark of the MHTGR-350 MW Core Design: Benchmark Definition", OECD Nuclear Energy Agency, NEA/NSC/DOC(2013), DRAFT (03/01/2013).
3. C. RABITI, A. ALFONSI, A. EPINEY, "New Simulation Schemes and Capabilities for the PHISICS/RELAP5-3D Coupled Suite", *Nuclear Science and Engineering*, Vol. 182 No. 1, pp. 104-118 (2016).
4. G. STRYDOM, et al., "Comparison of the PHISICS/RELAP5-3D Ring and Block Model Results for Phase I of the OECD/NEA MHTGR-350 Benchmark", *Nuclear Technology*, Vol. 193, pp. 15-35 (2015).
5. G. STRYDOM, F. BOSTELMANN, "IAEA Coordinated Research Project on HTGR Physics, Thermal-Hydraulics, and Depletion Uncertainty Analysis. Prismatic HTGR Benchmark Definition: Phase I", INL/EXT-15-34868 (2015).
6. P. ROUXELIN, G. STRYDOM, "IAEA Coordinated Research Project on HTGR Uncertainties, Comparison of the super cell options for Ex I-2c and coupling with the PHISICS-RELAP5-3D core model for Ex II-1", INL/EXT-15-36306 (2016).
7. B. TYOBEKA, K. IVANOV, A. PAUTZ, "Utilization of Two-dimensional Deterministic Transport Methods for Analysis of Pebble Bed Reactors", *Annals of Nuclear Energy*, 34, pp. 396-405 (2007).